www.czasopisma.pan.pl PAN POLSKA AKADEMIA NAUK www.journals.pan.pl

Arch. Metall. Mater. **67** (2022), 2, 703-717

DOI: https://doi.org/10.24425/amm.2022.137809

AZIZEH MAHDAVI[1], ALI REZA MASHREGHI[1*], SAEED HASANI[1], MOHAMMAD REZA KAMALI[1]

REOBSERVATIONS OF RECRYSTALLIZATION AND ITS EEFFECT ON MECHANICAL AND MAGNETIC PROPERTIES IN A SEVERELY COLD-ROLLED Ni-BASED SOFT MAGNETIC ALLOY

Despite of extensive researches for decades, there are many unclear aspects for recrystallization phenomenon in the cold rolled Ni-based alloys. Hence, different thermal cycles were conducted in order to determine microstructural evolutions and its effect on the magnetic and mechanical properties of a 90% cold-rolled thin sheet of a Ni-Fe-Cu-Mo alloy (~80 μm). The obtained results revealed that the recrystallization was started at a temperature of 550°C and was completed after 4 hours. An increase in the number of annealing twins was observed with an increase in annealing temperature, which was due to a bulging and long-range migration of grain boundaries during the discontinuous recrystallization. Ordering transformation occurred in the temperature range of 400-600°C and as a result, hardness, yield strength, and UTS were increased, while with an increase in the annealing temperature these mechanical properties were decreased. Maximum toughness was obtained by annealing at 550°C for 4 hours, while the highest elongation was obtained after annealing at 1050°C, where other mechanical properties including toughness, hardness, yield strength, and UTS were decreased due to the grain growth and secondary recrystallization. Moreover, coercivity and remanence magnetization were decreased from 4.5 Oe and 3.8 emu/g for the cold rolled sample to below 0.5 Oe and 0.15 emu/g for the sample annealed at 950°C, respectively.

Keywords: Ni-based alloy; Soft magnet; Recrystallization; Microstructural characterization; Mechanical properties; Coercivity

1. Introduction

The soft magnetic alloys are used in a wide range of commercial and industrial products [1]. Among these alloys, the Ni-Fe-based alloys are particularly utilized in the various industries such as electrical industry [2-5]. For instance, these alloys are used in rotor and stator laminations, stepping motors, relay parts, audio heads, high quality transformers, unipolar pulse transformers, magnetic shielding, magnetic amplifiers, inverters, converters, and other saturable reactors [1,6], which is due to their excellent magnetic properties including low core loss, very low coercivity (H_c), and high initial and maximum permeabilities [7,8].

These alloys have been developed in three categories; (a) alloys containing about 30 wt.% Ni with a curie temperature close to room temperature and maximum resistivity; (b) alloys containing about 50 wt.% Ni with a maximum saturation magnetization (M_s); and (c) alloys containing about 80 wt.% Ni with anisotropy and magnetostriction constants close to zero [9] and maximum permeability [10-13]. Hence, a numerous studies [14-17] have been done to develop this class of the alloys. As a result, it is known that the addition of alloying elements (i.e. Cu [5,6,18,19], Mo [5,6,18,19], Cr [5,6,18], Co [6], and Mn [6,18,19]) can be as one of the most effective method to improve the mechanical and magnetic properties of these alloys. On the other hand, it is notable that to achieve the optimum magnetic properties, amounts of the electronegative (N, O, and S) or electropositive (Al, Mg, Ca, and Ti) elements as well as the impurities with a small atomic radius (i.e. C and N) should be minimal [9]. Therefore, the permalloys are annealed in an inactive atmosphere such as argon or hydrogen [20,21].

Magnetic properties of the ferromagnetism materials is dependent to the behavior of magnetic domains in an external magnetic fields, which can be affected by various parameters such as magnetocrystalline anisotropy and magnetostriction [10,22], grain size [23,24], inclusions [25], texture [22,26], production processes [27,28], and the presence of alloying elements [29-34]. Therefore, by controlling these parameters, a wide range of magnetic properties can be created in this category of alloys [1,6]. In this case, some articles have reported

[1] YAZD UNIVERSITY, DEPARTMENT OF MINING AND METALLURGICAL ENGINEERING, 89195-741, YAZD, IRAN

* Corresponding author: amashreghi@yazd.ac.ir

that the order-disorder is as one of the main effective parameters on the magnetic properties in these alloys, so that if a critical degree of SRO forms, both the anisotropy energy and magnetostriction constants are simultaneously reduced to small values (near to zero) [4,6,20]. On the other hand, it is reported that the rate of ordering transition in these alloys is very slow, so that to approach the maximum value of order phase ($L1_2$), an annealing process at 450°C for one week is required [35]. Numerous researchers have focused on this transformation and the obtained results revealed that by adding alloying elements such as Cu [5,6,18,19], Mo [5,6,18,19], Cr [5,6,18], and V [35], the ordering kinetics slowed down, which leads to decrease in the degree of long-range order. Moreover, it is shown that the addition of Mo and/or Cu can reduce the cooling rate required to achieve magnetocrystalline anisotropy (K_1) = 0 [36,37]. On the other hand, mechanical properties of these alloys are affected by structural evolutions such as texture evolution [1] due to the changing process parameters [37].

Although, extensive researches for decades have been done, but there are many unclear aspects for recrystallization phenomenon in cold rolled Ni-based alloys and its dependent mechanical and magnetic properties. Hence, the Ni-14Fe-5Cu-4Mo ultra-thin foils are produced by thermomechanical method in the present study. Then, recrystallization and its effect on the mechanical and magnetic properties in this severely cold-rolled Ni-based soft magnetic alloy are investigated.

2. Materials and methods

The material under study was a Ni-Fe-Cu-Mo alloy with the chemical composition as follows: 14 wt% Fe, 5 wt% Cu, 4 wt% Cu and balanced with Nickel, which was measured by the atomic absorption spectrometry (AAS). The composition of the used alloy is listed in table 1. The alloy was melted in a vacuum furnace with the use of pure charge materials (99.99%). The as-cast ingots were homogenized by annealing at 1100°C for 10 h under high purity Ar atmosphere. Then, the homogenized ingots were subjected to hot rolling in a temperature range of 1050-1150°C to prepare sheets with the thickness of 1mm (~90% reduction). After eliminating the surface layer using sand paper grinding, the hot-rolled sheets were annealed at 950°C for 4 h under high purity Ar atmosphere. Then, these sheets were subjected to cold rolling to achieve a 92% reduction in thickness (80 μm).

TABLE 1

Chemical composition of the studied alloy in wt.%

Element	Fe	Cu	Mo	Other elements	Ni
wt.%	14.49	4.94	3.94	<0.01	Balanced

The cold rolled ultrathin foils were annealed in a high purity vacuum at a temperature range from 400°C to 1100°C for various times (30, 120, and 240 min), followed by quenching in the cooled Ar atmosphere. Phase analysis was performed by using XRD (X'Pert MPD Philips diffractometer) method, fitted with diffracted-beam monochromator set for cobalt Kα (λ = 0.17890 nm) radiation operated at 40 kV and 40 mA in the back-reflection mode and a step size of 0.02°. Microstructural observations were carried out using an OM (Olympus PMG3) and a FE-SEM (MIRA3 TESCAN). For this purpose, the surfaces of samples were mechanically polished and then were etched in 5 g $FeCl_3$ + 40 ml Ethanol + 10 ml HCl (37%) solution. Also, mechanical properties of the samples were measured using tensile (Instron 5586) and microhardness (MH3 KOOPA) tests. The sub-size flat tensile test specimens used in the tests is plotted in Fig. 1. Three tensile specimens were tested for each condition and the average was reported as a result. Tensile tests were carried out at room temperature in the rolling direction by an initial stain rate of 0.001 s^{-1}. Moreover, the fracture surface were analyzed using a FESEM. Microhardness was measured under a load of 1 N for 10 s owing to low thickness of samples and the average of 5 measurements with 2 mm distance between each point on the surface of samples was considered in calculations.

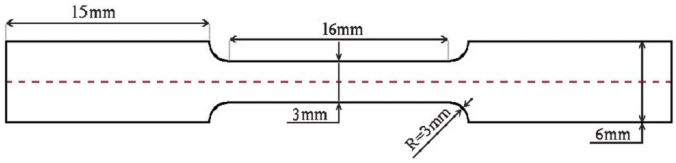

Fig. 1. Schematic of the used sub-size tensile test specimen

3. Results

3.1. Microstructural observation and phase analysis

3.1.1. Recrystallization

Figs. 2(a) and (b) show OM micrographs of surface and cross-sectional views of the hot rolled sample. As seen, the microstructure characteristic of the sample with different positions is almost the same. The presence of equiaxed grains in the microstructure confirms the occurrence of dynamic recrystallization (DRX) during the hot rolling process at temperature range of 1050-1150°C. Fig. 2(c) represents microstructure of elongated grains of the cold rolled sample, which shows the grain boundaries and deformation bands. It is accepted that during the severe plastic deformation, regions with various directions are developed by strain heterogeneity taking place due to compatibility requirements of neighboring grains or any intrinsic instability of grain during plastic deformation [38]. These grain subdivision or grain fragmentation (ranging from nm to mm scale) can produce various orientations inside the grains (as seen in Fig. 2(c)). The coarsest form of grain subdivision are deformation bands which simply are recognizable by optical microscope, while narrow regions between deformation bands are called transition bands, which can be clear or unclear inside the microstructure [39]. Moreover, deformation bands are formed on various slip systems [40]. In fact, deformation leads to a stored energy which act as

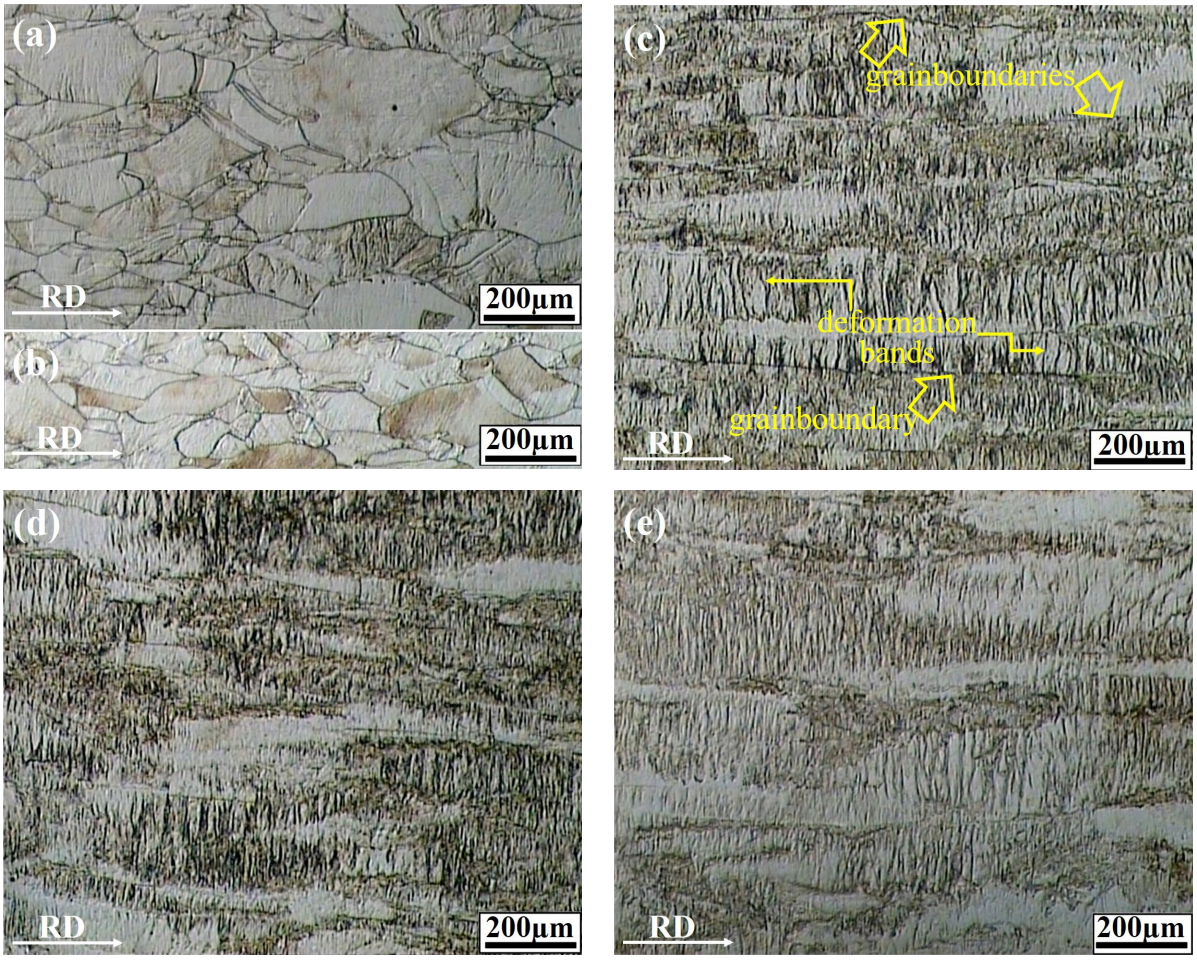

Fig. 2. OM micrographs related to (a) surface and (b) cross section of the hot rolled samples, and micrographs of (c) the cold rolled sample and the samples annealed at (d) 450ºC and (e) 500ºC for 4h

driving force for recovery and recrystallization during annealing [41-43]. However, it is notable that elongation of grains along the rolling direction leads to increasing the density of dislocations distribution around the grain boundaries, which can prevent to distinguish between boundaries in microstructure [17].

Figs. 2(d) and (e) show the microstructures of the samples annealed at 450 and 500°C for 4h. These microstructures are similar to microstructure of the cold rolled sample (Fig. 2(c)), indicating that recrystallization has not yet begun. On the other hand, it is well known that microstructural evolutions during recovery process are not significant and take place in a small scale. These changes usually do not affect the boundaries of deformed grains [40]. However, shear bands are shown with higher resolution in Figs. 2(d) and (e) due to the decreasing of dislocations density during the recovery. However, shear bands, independent of the grain structure, often occur at 35 to 45° to the rolling plane and parallel to the transverse direction [44,45].

Metals/alloys with cubic crystal structure are deformed by slip and twinning mechanisms [46], where the slip is the main plastic deformation mechanism for metals/alloys with a high stacking fault energy (SFE) [47,48]. The SFE of Ni-Fe alloys is reported in the range of 70 mJ/m^2 [49], and therefore the main plastic deformation mechanism in these alloys is slip.

Fig. 3 shows the shear micro-bands and fish bone pattern in the cold rolled sample. As seen, at high strains, shear bands form colonies with a set of parallel bands (Fig. 3(a)) and/or with a pattern known as fish bone pattern (Fig. 3(a)), which is in good agreement with that obtained by others [50].

Fig. 4 shows microstructure of the samples annealed at 550°C for 10 and 30 min. These micrographs reveal that recrystallization begins at 550°C.

Recrystallization process occurs by either a continuous or discontinues mechanism [40]. The continuous recrystallization is based on the diffusion and rearrangement of dislocations to form sub-grains, which is followed by coalescence of these sub-grains and converting to a high angle boundary. In this case, the driving force to form a strain-free grain is decreasing the strain energy due to replacement of several sub-grain boundaries by a single high-angle boundary [51,52]. While, in discontinues recrystallization, the new strain-free grains (crystallized grains) are formed in certain parts of the sample, such as initial grain boundaries. The subsequent growth of these grains leads to promote the consumption of deformed and/or recovered microstructure, so that before the end of the recrystallization, the microstructure is divided to the recrystallized and non-recrystallized grains [40,53]. As presented in Fig. 4, the occurrence of discontinuous

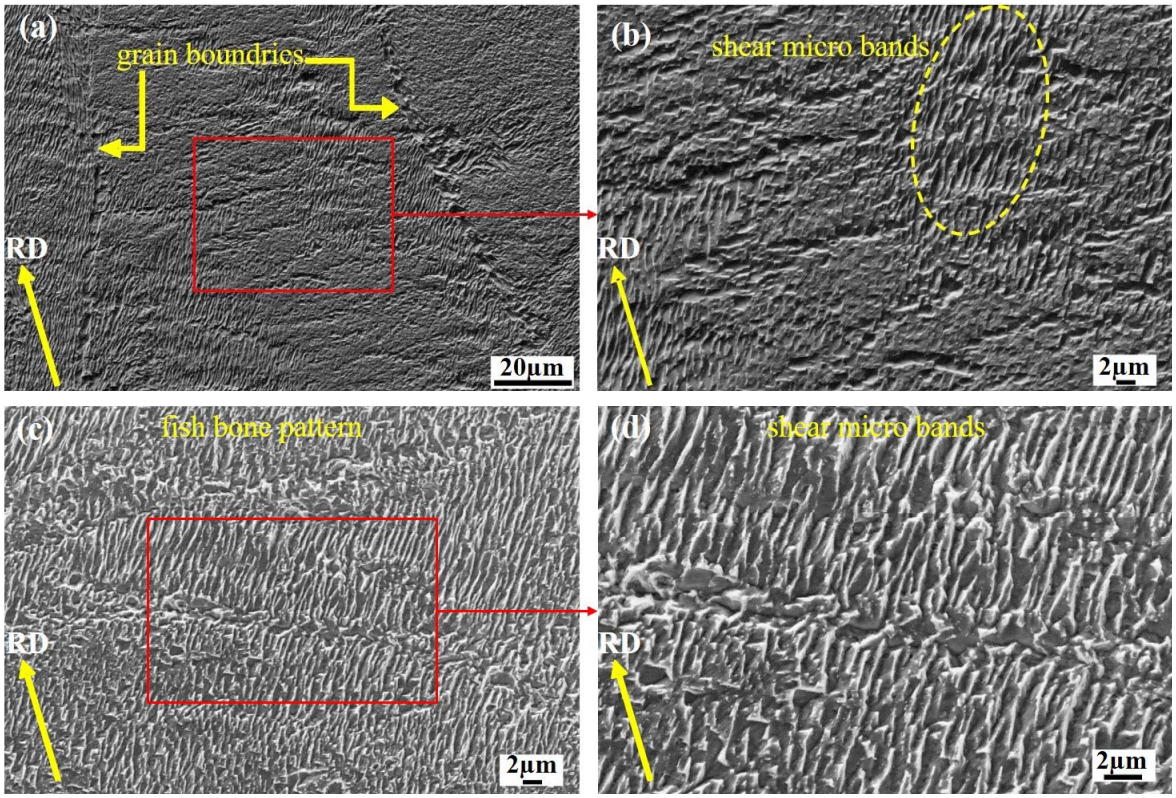

Fig. 3. FE-SEM micrographs of (a) shear micro bands, (b) higher magnification of (a), (c) fish bone pattern and (d) higher magnification of (c), formed in the cold rolled sample

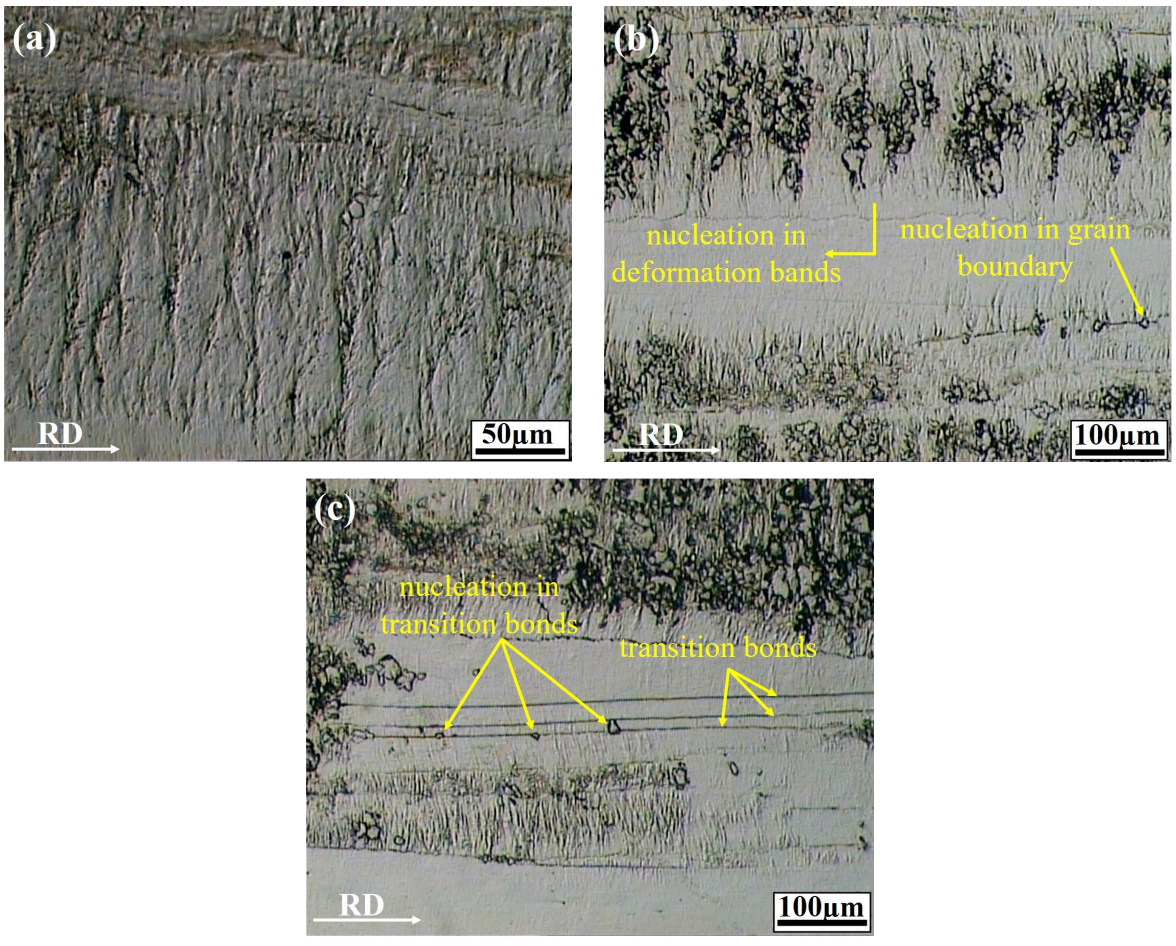

Fig. 4. OM micrographs related to the samples annealed at 550ºC (a) for 10 min, (b) and (c) for 30 min

recrystallization is proved in this alloy. As seen, nucleation of the recrystallized grains originates at inhomogeneities in the deformed microstructure, such as deformation bands (Fig. 4(b)), transition bands (Fig. 4(c)), or at pre-existing microstructural defects (i.e. grain boundaries (Fig. 4(b))). In addition, it can be seen that average size of the crystallized grains varies in different inhomogeneities regions depending on the amount of energy stored in them.

Fig. 5 represents microstructure of the samples annealed at 550°C for 2 and 4 hr. As observed in Fig. 5(a), no recrystallization occurs in some regions, while with the increasing annealing time to 4 hr, recrystallization process occurs in the whole sample (Fig. 5(b)). Also, Fig. 5(b) shows that in the areas where the recrystallization started in the previous stages, the grain growth stage has now started.

Fig. 6 shows that with the increasing annealing temperature to 600 and 700°C, not only recrystallization occurs at a higher rate but also larger grains is formed, which is in good agreement with that obtained by others [54,55]. Furthermore, annealing twins are observed in these samples, which are indicated by yellow arrows. As reported, these twins could be formed during recovery [56], recrystallization [57] and/or consequent grain growth [58].

It is observed that the twins become larger and wider inside the recrystallized grains with an increase in annealing temperature up to 950, 1000 and 1100°C (Fig. 7). As seen in Fig. 7, the annealing twins are formed in parallel layers, where in FCC metals/alloys, these layers are connected by {111} plains with the coherent boundaries [40].

It is reported that in the grain growth stage of ultra-thin foils, if grain size is sufficiently increased (more than 0.1 of thickness) [42], the “thermal grooving” can be appeared due to the intersection of the grain boundary with the free surface [59]. This phenomenon can greatly reduce the grain growth rate. Therefore, at the higher temperature range, where the grains are large enough, these grooves can form at the intersection of the grain boundary with the free surface of sample. Fig. 8 shows the formed thermal grooving for the samples annealed at 1000 and 1100°C. It is notable that these micrographs are prepared without any polishing and etching. Grain boundary grooves act as barriers to the grain boundary movement and decelerate the grain growth [60].

The variation of grain size versus annealing temperature is shown in Fig. 9. As seen, the grain growth rate is reduced from 900°C that it is due to the formation of these grooves. However, remarkable grain growth is observed at above 1000°C (Fig. 8(b)),

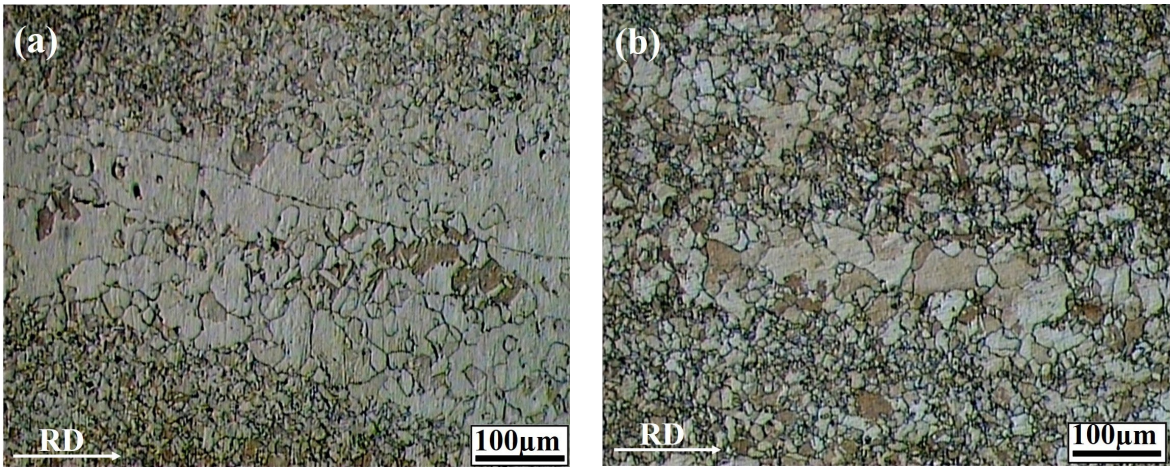

Fig. 5. OM micrographs related to the samples annealed at 550ºC for (a) 2 and (b) 4 hr

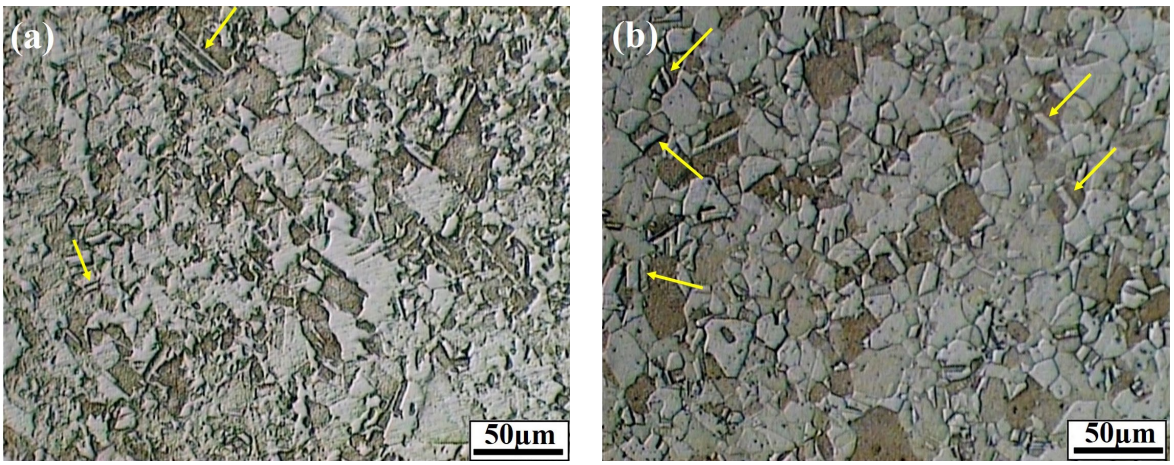

Fig. 6. Microstructure of the samples annealed at (a) 600 and (b) 700ºC for 4h (some twins are indicated by yellow arrows)

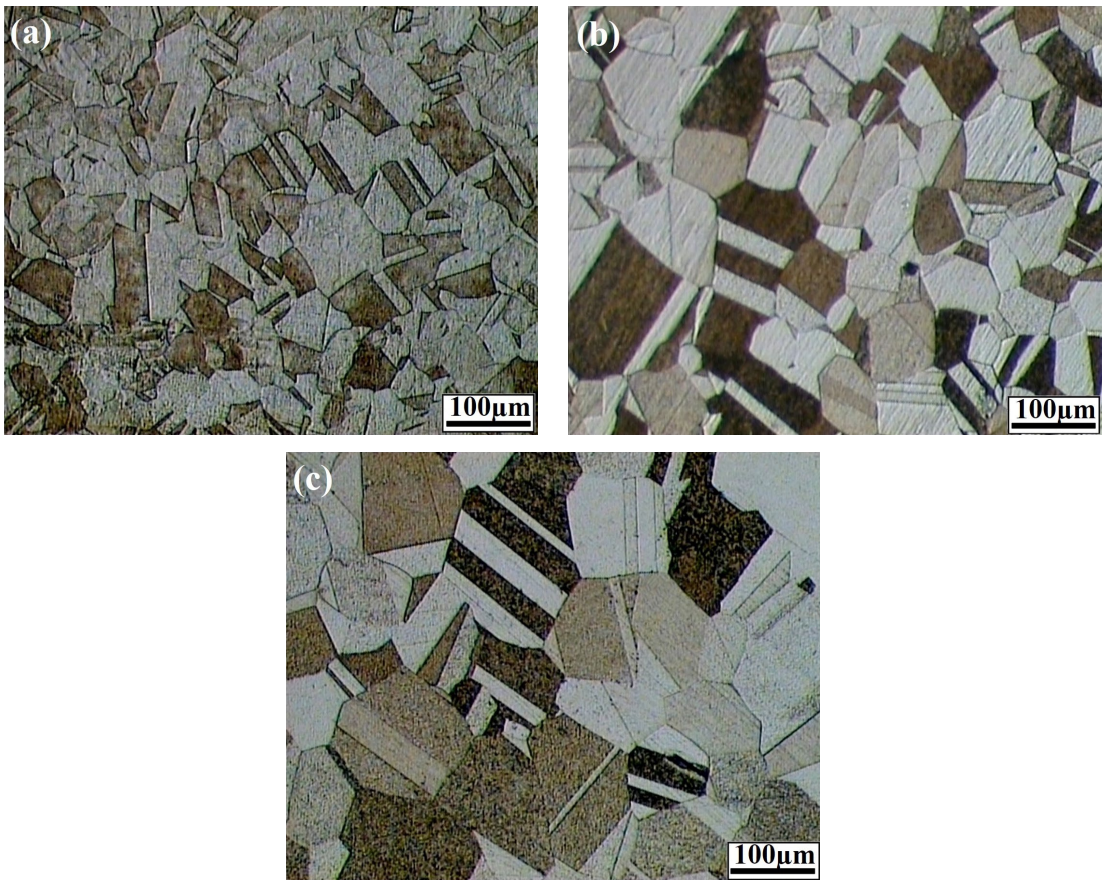

Fig. 7. Recrystallized grains and annealing twins formed in the samples annealed at (a) 950, (b) 1000, and (c) 1100ºC for 4 hr

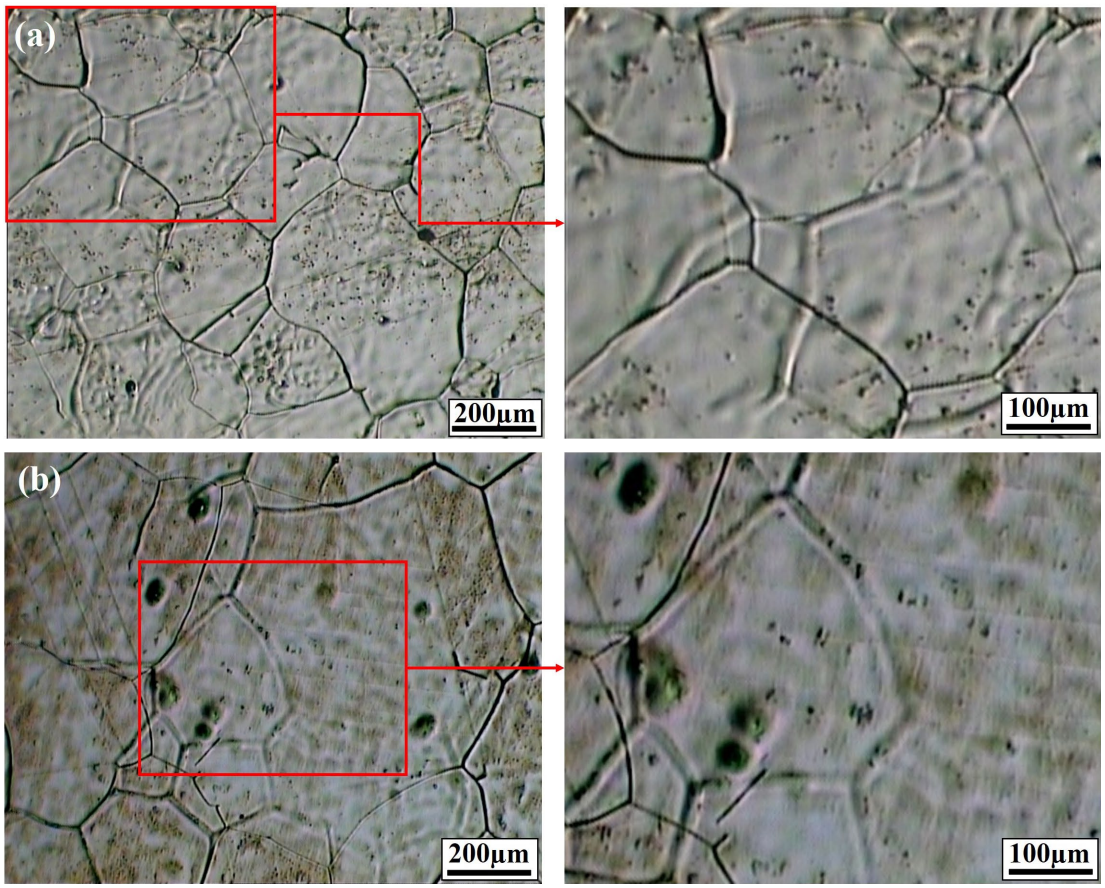

Fig. 8. Optical micrographs of the samples annealed at (a) 1000 and (b) 1100ºC for 4h without any polishing and etching

which is attributed to secondary recrystallization. However, the grooves are still observed inside this structure.

This remarkable grain growth usually occurs at temperatures higher than temperature associated with initial recrystallization. Typically the driving force for secondary recrystallization has been assumed to be due primarily to surface energy considerations only and not related to prior work or stored strain energy [60,61]. Therefore, inhibition of normal grain growth by grooves can be a main factor for the occurrence of abnormal grain growth phenomenon (secondary recrystallization). The significant increase in the average grain size at 1100°C (Fig. 9) confirms the occurrence of secondary recrystallization.

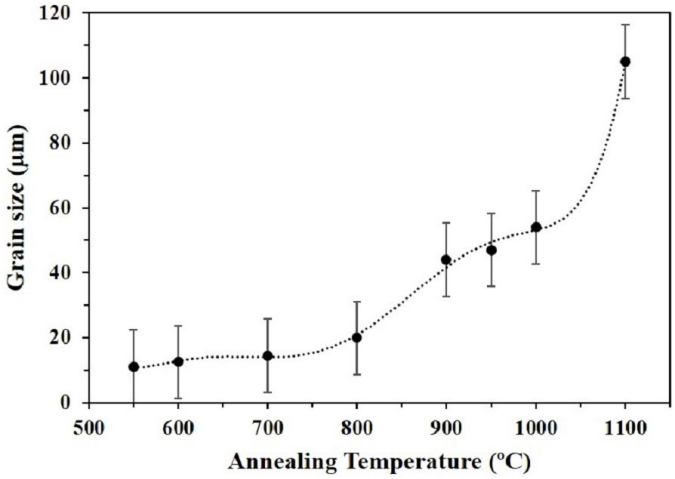

Fig. 9. The variation of grain size versus annealing temperature

3.1.2. Ordering transition

The ordering transition is the main parameter affecting other transformation (i.e. recovery, recrystallization, and grain growth), and mechanical/magnetic properties [62-64]. For instance, it is reported that kinetics of recrystallization in a semi hard magnet Fe-50Co-10V alloy is slowed down as a result of this transition [65,66], due to the restriction of the dislocations and grain boundaries mobility. As reported, ordering transition occurs in the temperature range from 300 to 600°C in this alloy [67], so that can be identified by using the XRD method. XRD patterns of the samples annealed at 400, 500, and 600°C for 4 hr are shown in Fig. 12. As seen, there are typical diffraction characteristic peaks of a single FCC phase (JCPDS card No. 03-065-0380) for all samples, which is in good agreement with binary phase diagram of Ni-Fe [68]. As demonstrated in Fig. 12, this superlattice reflections can be observed at $2\theta = 42°$ (as indicated by an arrow) for the samples annealed at this temperature range, which is due to the formation of long-range ordered (LRO) phase. On the other hand, formation of the short-range order (SRO) phase also occurs in this temperature range, which can greatly affect the properties [64].

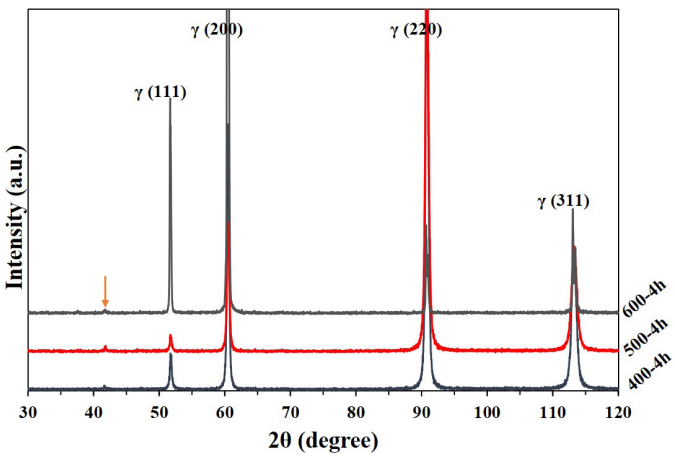

Fig. 10. XRD patterns of the samples annealed at various temperatures

3.2. Mechanical properties assessment

3.2.1. Microhardness

Fig. 11 represents microhardness evolutions (HV) of the cold rolled sample and the samples annealed from 400 to 1100°C as a function of annealing times. As seen, microhardness is increased with annealing temperature up to 400-450°C. After that, microhardness decreases with annealing temperature up to ~600-800°C. No significant change is observed with further increase in annealing temperature to 1100°C.

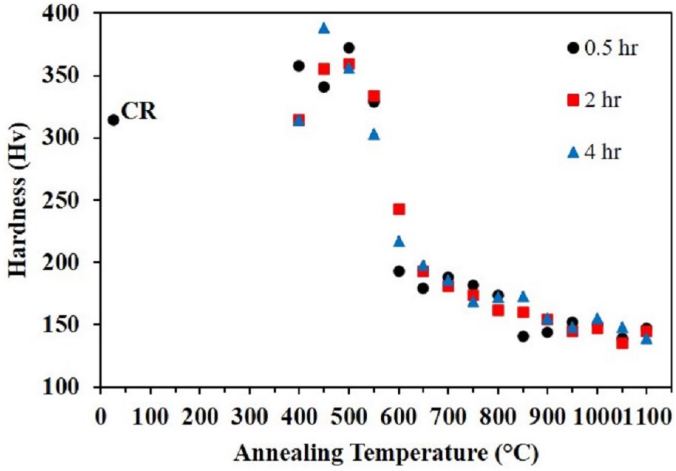

Fig. 11. Microhardness evolutions of the cold rolled sample and the samples annealed from 400 to 1100°C for various times (CR: cooled rolled sample)

XRD patterns represented in Fig. 10 shows that the ordered phase is present in the samples annealed between 400 and 600°C, so that the maximum degree of ordering in the studied alloy is achieved by annealing at ~500°C. As seen, microhardness is increased due to an increase in the degree of LRO/SRO by annealing at 400°C, which is in good agreement with that obtained by others [40,69]. An ordered structure contains superdislocations, which consist of two unit dislocations separated by a strip of antiphase boundaries (APBs). Hence, microhardness can be increased in the ordered structure. On the other hand, the mi-

crostructural observations (Fig. 4) revealed that recrystallization and formation of fine grains occurs at 550°C, which can become larger with an increase in annealing time, which is in good agreement with that shown in Fig. 11. Hence, microhardness decreases by an increase in annealing time from 30 min to 4 hr.

3.2.2. Yield strength (YS) and Ultimate tensile strength (UTS)

Fig. (12) shows the YS and UTS of the samples annealed from 400 to 1100°C as a function of annealing time, respectively. A similar trend is observed in these two figures with the microhardness changes (Fig. 11). As seen, these both YS and UTS increase with annealing at 450°C and decreases again at higher annealing temperatures. Since recrystallization has not yet begun at 400°C, ordering transition is the cause of this increase. It is notable that at temperatures lower than 550°C, various transformations including recovery and ordering are occurring simultaneously. Therefore, the evolutions observed at these temperatures for various annealing times are not regularly. For instance, the YS increases with increasing annealing time up to 2 hr at 450° C, but with 4 hr of annealing at this temperature decreases again, which can be the result of more recovery in this sample. Similar behaviors have been reported by other researchers [40].

However, a sharp decrease in the YS and UTS in the temperature range of 500-550°C can result in the onset of recrystallization and a decrease in the degree of order. By increasing the annealing temperature (from 550 to 1100°C) and completing the recrystallization process and starting the grain growth, reducing the YS and UTS seems reasonable.

3.2.3. Elongation and toughness

Elongation and toughness of the samples annealed at various annealing temperatures for 4 hr are illustrated in Figs. 13(a) and (b), respectively. As seen. These mechanical properties are minimum for the cold rolled sample due the high dislocation density. Although the elongation and toughness do not change significantly with the annealing up to 500°C, which can be due to the interaction between the ordering transformation (as SRO [70]) and recovery [40], these properties are greatly enhanced with increasing the annealing temperature to 550°C. As mentioned in the section 3.1.1, the fine equiaxed grains are formed at this temperature due to the beginning of recrystallization. However, it is observed that the trend of changes in elongation and toughness is reversed with an increase in the annealing temperature above 600°C, so that the elongation shows an increase in trend with the increasing annealing temperature (Fig. 13(a)), while the toughness has a downward trend with the increasing annealing temperature (Fig. 13(b)). It is accepted that the elongation is increased by recrystallization as well as disappearance of ordered phase above 600ºC. Also, the results show that the toughness, the area under the stress-strain curve, of the samples annealed at temperatures above 600°C decreases (Fig. 13(b)). It is worth noting that the maximum toughness is depends to the elongation and strength, simultaneously. It can be seen that with increasing annealing temperature from 600°C, the amount of strength reduction (Fig. 12) is greater than the amount of elongation increase (Fig. 13(a)). The maximum toughness is achieved for the sample annealed at 550°C, where the fine recrystallized grains are formed. However, the cold rolled sample has the minimum toughness due to the both high dislocation density and cold rolling residual stresses. On the other hand, it is known that ordering transition affects these mechanical properties [71], so that in the disordered structure, sharp slip bands with large offsets on the primary system are observed in the early stages of deformation, and at later stages sharp bands appear on other systems. In the ordered condition, the unit dislocations cannot cross-slip individually and also it is unlikely that cross-slip of the associated pair can occur, because this would require the second dislocation to follow exactly in the wake of the first one. Therefore, it is expected that the mobility of the dislocations be decreased in the ordered condition. Nevertheless, the obtained results in the present study show that recrystallization and grain growth process are more effective than ordering.

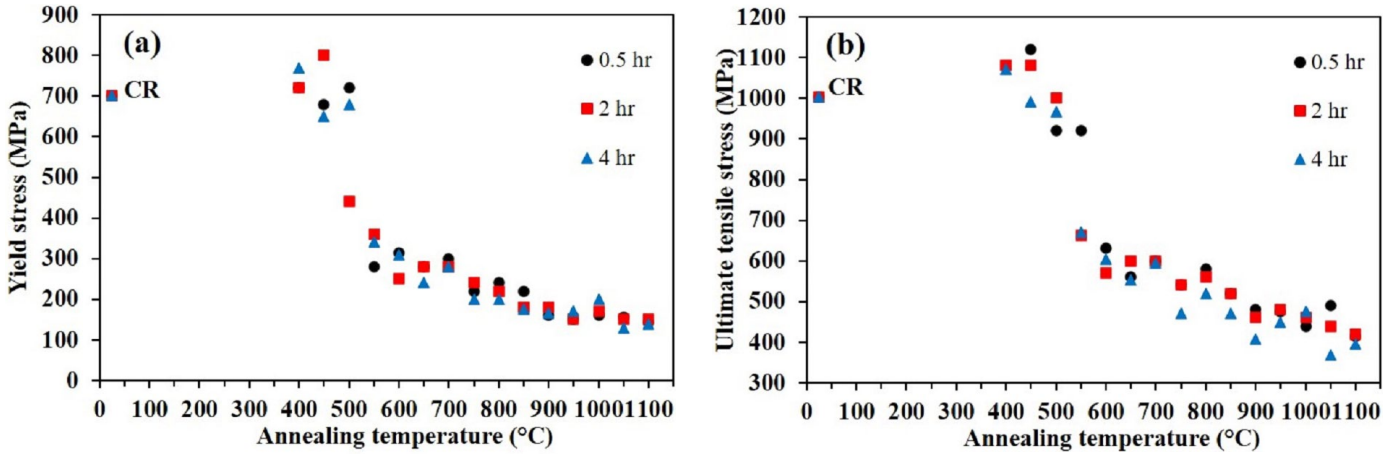

Fig. 12. (a) YS and (b) UTS evolutions of the cold rolled sample and the samples annealed from 400 to 1100°C for various times (CR: cooled rolled sample)

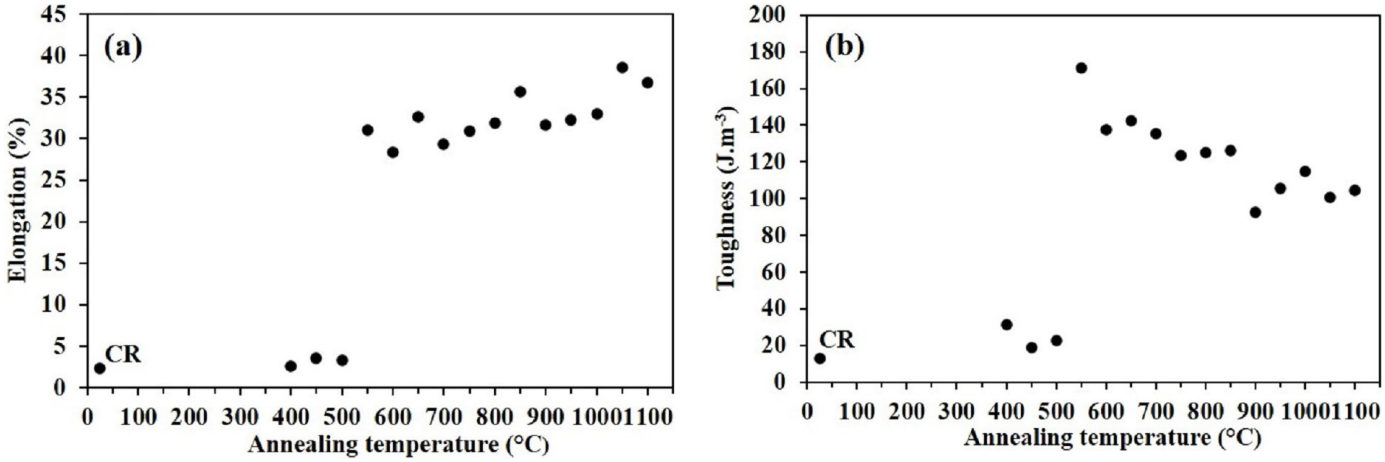

Fig. 13. (a) elongation and (b) toughness evolutions of the samples annealed from 400 to 1100°C for 4 hr (CR: cooled rolled sample)

3.2.4. Fractography

Fractography of the fractured samples shows in Fig. 14. As seen, necking is observed for all samples even for the cold rolled sample (Fig. 14(a)); indicating a ductile fracture mechanism. This mechanism, which is well known as "cup and cone", is shown in ductile fracture surface in uniaxial tensile test for polycrystalline metals as demonstrated by Orowan [72]. When uniaxial tensile loading is applied to a ductile material, deformation becomes localized on a small part of the gauge length of the specimen,

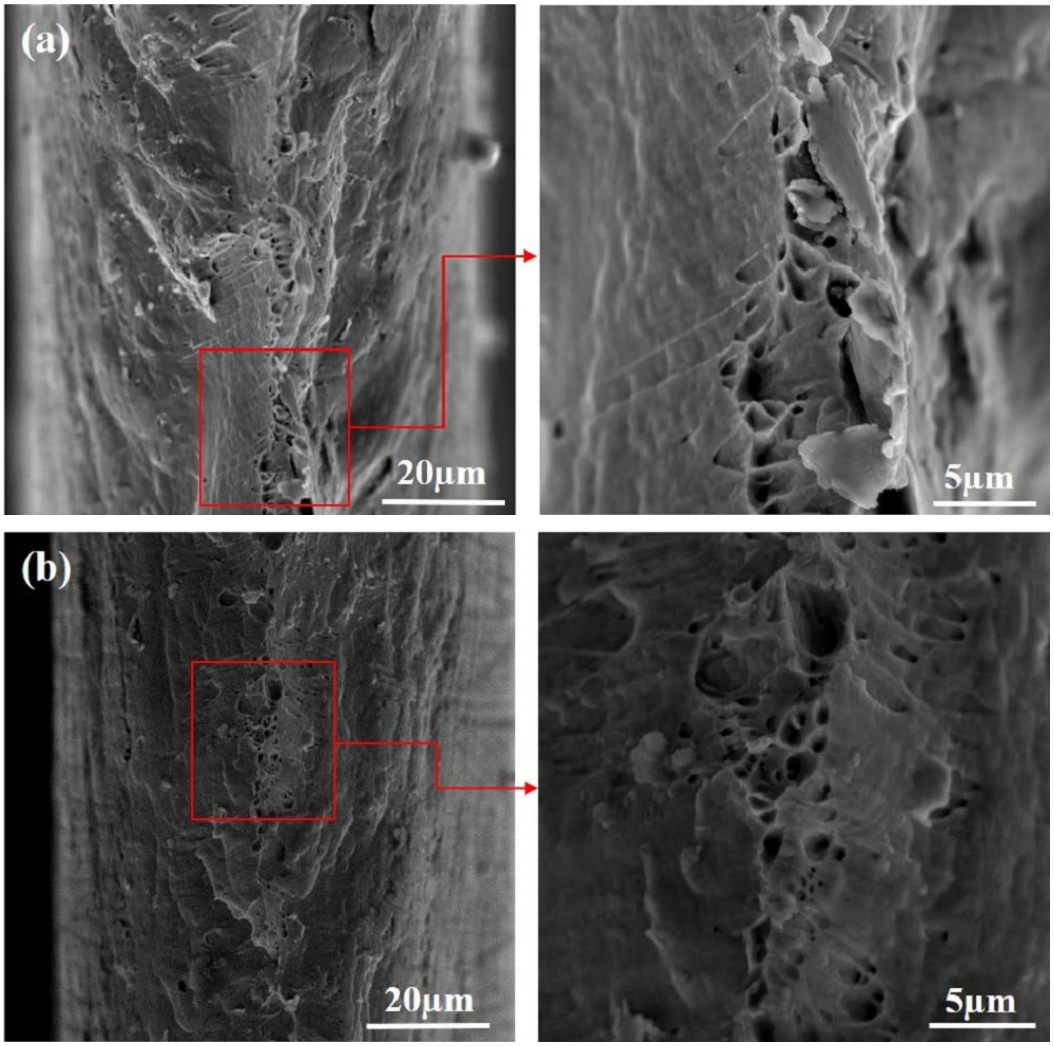

Fig. 14. SEM fractography of (a) cold rolled sample and annealed samples at (b) 550°C for 0.5 hr, (c) 550°C for 4 hr, (d) 750°C for 4 hr, and (e) 1100°C for 4 hr

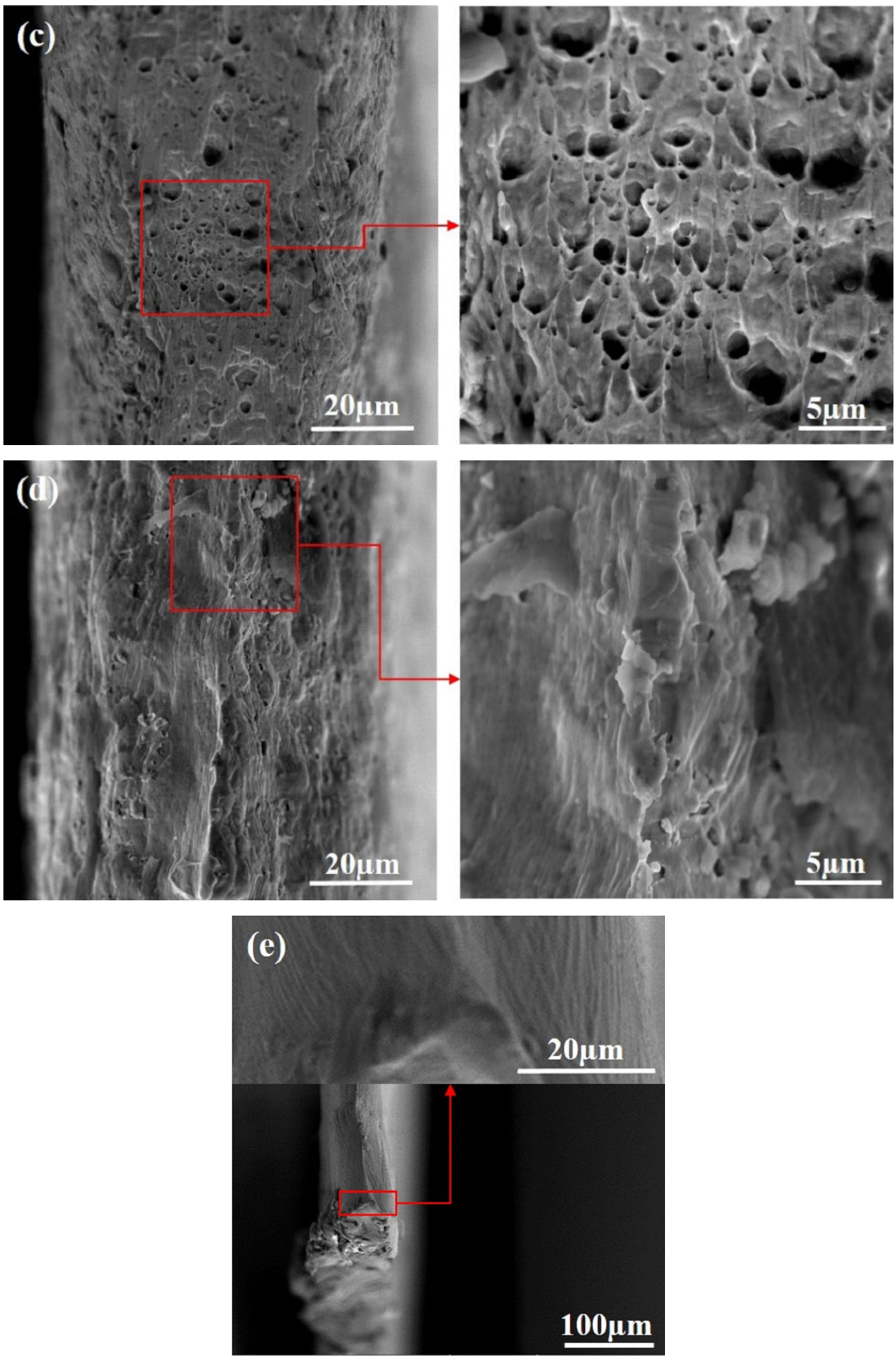

Fig. 14 continued. SEM fractography of (a) cold rolled sample and annealed samples at (b) 550°C for 0.5 hr, (c) 550°C for 4 hr, (d) 750°C for 4 hr, and (e) 1100°C for 4 hr

and necking begins and therefore micro-voids are formed in grain boundaries [73]. Most of fracture energy is consumed by micro-voids growth [74], so that fracture energy is increased by increasing depth and width of micro-voids [75]. Therefore, the morphology of fracture surface is dependent to the loading direction [76]. For instance, in the studied specimens, as the deformation continues to higher strains and formation of necking, the load bearing area becomes so small and then fast propagation occurs on a plane inclined to the fracture surface by 45º (shear lip) (Fig. 14). Orowan [72] reported another fracture mechanism,

which is based on the formation of a polyhedral transverse channel in the neck. It is well-known that in plane-strain tension, the deformation localizes along the characteristics (slip lines) of perfect plasticity; these are aligned along lines inclined at 45° with respect to the direction of tension. In addition, the growth and coalescence of micro-voids can occur on the maximum shear stress plane and due to unequal triaxial stresses, some dimples are elongated in one or other directions. These appearances are the characteristics of a typical ductile fracture [77,78].

Fig. 14(b) represents a small number of fine dimples in the center of the sample without any cleavage facets, which confirms the beginning of recrystallization in the sample annealed at 550°C for 0.5 hr. Furthermore, a different morphology (a terraced appearance) is also observed in this fractography. This appearance suggests that the failure on the shear planes is occurred due to the Orowan's alternating slip mechanism. This mechanism is known by the formation of a polyhedral transverse channel in the neck. By increasing the annealing time at 550°C to 4 hr, a significant increase in dimples is observed (Fig. 14(c)), which is due to the recrystallization progress and formation of the fine recrystallized grains. The Orowan's alternating slip mechanism is the dominant failure mechanism in the sample annealed at 750°C for 4 hr (Fig. 14(d)). As the annealing temperature increases, the grain size increases, and therefore the density of grain boundaries decreases, thus the formation of dimples can be reduced, so the predominant mechanism of fracture is the Orowan's alternating slip mechanism (Fig. 14(e)).

3.3. Magnetic properties

Magnetic properties of the 90% cold rolled sheet of Ni-14Fe-5Cu-4Mo (wt.%) permalloy and its annealed sheets at various temperatures were investigated by VSM. The changes in the magnetic parameters extracted from M-H loops, are shown in Fig. 15. It is acceptable that magnetic properties are divided into two groups: structure-insensitive and structure-sensitive. The M_s and the Curie temperature are the two prominent structure-insensitive properties, while the remanence magnetization (M_r) and coercivity (H_c) are structure-sensitive. As seen, despite the M_s (Fig. 15(a)), the M_r and H_c change during the annealing process (Fig. 15(b) and (c), respectively). As seen, maximum values of the M_r and H_c are observed for the cold rolled sample due to shape, stress, and cold rolling anisotropies and elongated grain boundaries as well as high dislocation density, while by annealing process, soft magnetic properties are improved due to the recovery, recrystallization, and grain growth as well as eliminating mentioned anisotropies.

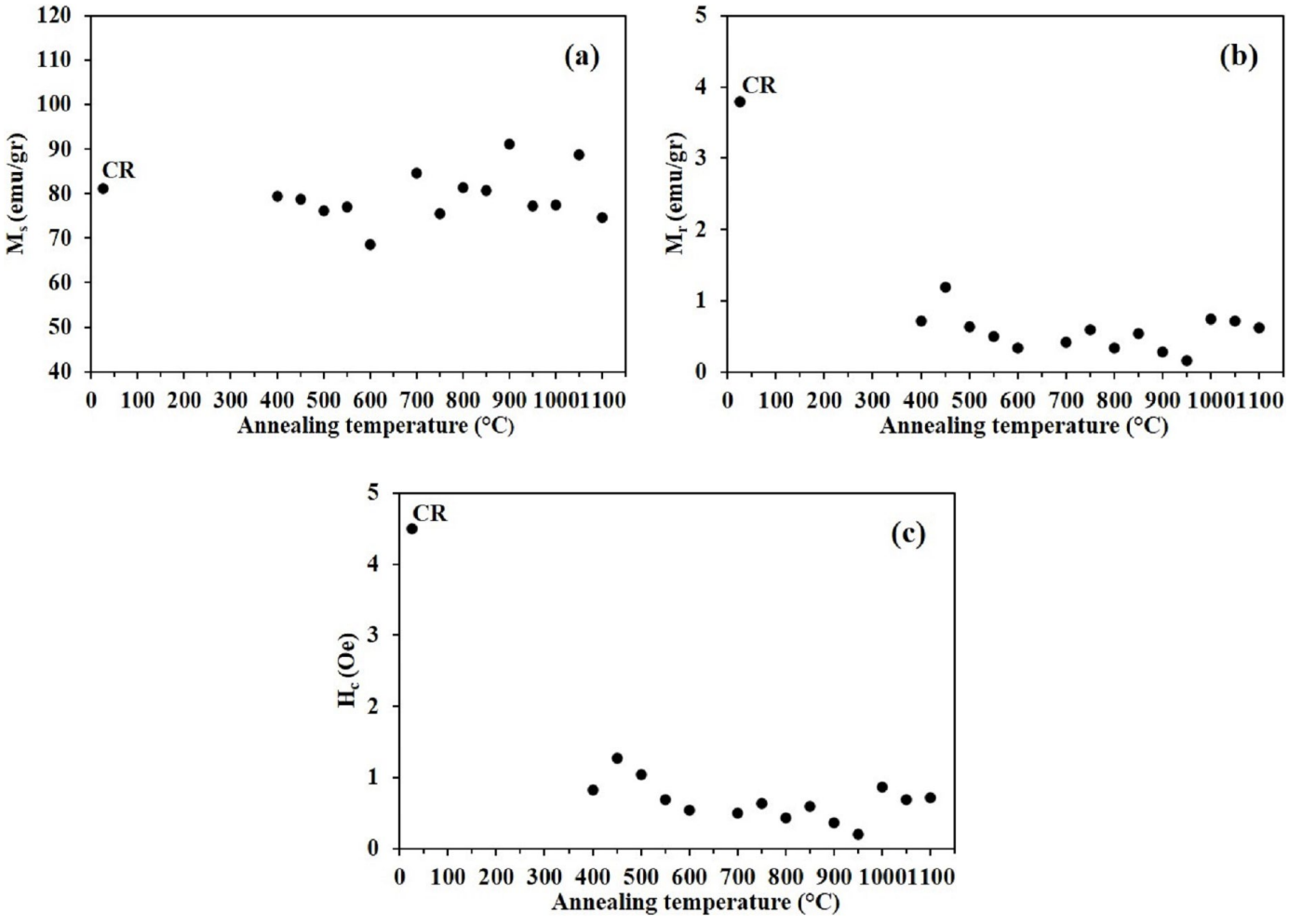

Fig. 15. Values of (a) M_s, (b) M_r, and (c) H_c for the cold-rolled and annealed specimens at various temperatures for 4 hr

Fig. 15(b) and (c) show that by annealing at 400°C, the M_r and H_c decrease and then increase again at 450°C, which can be due to the formation of ordered structure. Similar results have been reported in previous research [26]. On the other hand, high angle boundaries (HAGBs) of the fine recrystallized grains, which are formed at 550°C-4 hr, act as barriers to the mobility of magnetic domains [79]. Therefore, this increment can be due to the beginning of recrystallization [23,26,80-82]. With initiation of the recrystallization at 550ºC and following grain growth up to 950ºC, grain boundaries reduce, which can lead to a decrease in H_c and M_r at this annealing temperature range, so that the minimum values of M_r and H_c are achieved by annealing at 950°C (Fig. 15(b) and (c)). However, the soft magnetic properties of this alloy are deteriorated again at higher annealing temperatures (above 950°C), which can be related to changes in texture components at these temperatures [20].

4. Conclusions

In the present study, the microstructural evolution occurring during the recrystallization process in a 90% cold-rolled thin sheet of a Ni-Fe-Cu-Mo alloy was clarified. In addition, the effect of order-disorder transition on the magnetic/mechanical properties of this alloy was investigated. The most important findings are as follows:

- Recrystallization process began at 550°C, particularly in deformation, transition, and shear bands, which are consistent with a discontinuous mechanism. By increasing the annealing temperature/time, the recrystallization progressed and then followed by the abnormal grain growth during the "secondary recrystallization" above 1000ºC.
- The "thermal grooving" phenomenon was taken place after annealing above 900ºC due to intersection of grain boundary and free surface, when approaching the grain size to the thickness of sample. The grooves acted as barriers to the mobility of grain boundaries, which results in reducing the grain growth rate.
- The ultra-thin foils annealed at temperatures lower than 550ºC had highest strength and hardness with minimum elongation. The mechanical properties including YS, UTS and hardness decreased due to the recovery, recrystallization, and grain growth by raising the annealing temperature above 550ºC.
- Appearance of necking, dimples, and shear lip in the fracture surfaces of tensile samples showed a ductile failure. Maximum number of dimples was observed in 550ºC – 4 h sample owing to finest microstructure. However, with raising annealing temperature higher than 700ºC, the number of dimples is reduced due to the grain growth and following secondary recrystallization, so that the predominant fracture mechanism in the samples annealed at high temperatures was Orowan's alternating slip.
- The values of M_r and H_c seem to have strong relationship with the grain size and order/disorder transformation. In the alloy, the ordering transition occurred within temperature range of ~400-550ºC. However, by annealing the cold-rolled sample, the soft magnetic properties was improved due to the removing the shape, stress and cold rolling anisotropies. The best soft magnetic properties (minimum of H_c and M_r) were achieved by annealing at 950ºC.

Data availability statement

The raw/processed data required to reproduce these findings cannot be shared at this time as the data also forms part of an ongoing study.

REFERENCES

[1] G. Chin, J. Wernick, Ferromagnetic Materials, North-Holland, 1980.

[2] T. Akomolafe, G.W. Johnson, The effect of sheet thickness on the magnetic properties of 77 wt% Ni permalloys, J. Mater. Sci. **24**, 349-354 (1989). DOI: https://doi.org/10.1007/BF00660979

[3] G.W. Elmen, Magnetic Properties of Perminvar 1, Bell Syst. Tech. J. **8**, 21-40 (1929). DOI: https://doi.org/10.1002/j.1538-7305.1929.tb02304.x

[4] R.M. Bozorth, Ferromagnetism, Van Nostrand, New York, 1951.

[5] R.D. Enoch, A.D. Fudge, High magnetic permeability in Ni-Fe alloys, J. Appl. Phys. **17**, 623-634 (1966). DOI: https://doi.org/10.1088/0508-3443/17/5/307

[6] K. Gupta, K.K. Raina, S.K. Sinha, Influence of process parameters and alloy composition on structural, magnetic and electrical characteristics of Ni-Fe permalloys, J. Alloys Compd. **429**, 357-364 (2007). DOI: https://doi.org/10.1016/j.jallcom.2006.11.048

[7] X.Y. Qin, J.G. Kim, J.S. Lee, Synthesis and magnetic properties of nanostructured γ-Ni-Fe alloys, Nanostructured Mater. **11**, 259-270 (1999). DOI: https://doi.org/10.1016/S0965-9773(99)00040-9

[8] W.D. Callister, D.G. Rethwisch, Materials science and engineering: an introduction, Wiley New York, 2013.

[9] E. du T. De Lacheisserie, D. Gignoux, M. Schlenker, Magnetism: Materials and Applications, 1st ed., Springer-Verlag New York, New York, 2005. https://www.springer.com/gp/book/9780387230009

[10] G. Couderchon, J.F. Tiers, Some aspects of magnetic properties of Ni-Fe and Co-Fe alloys, J. Magn. Magn. Mater. **26**, 196-214 (1982). DOI: https://doi.org/10.1016/0304-8853(82)90152-4

[11] G.A.V. Sowter, Soft magnetic materials for audio transformers: History, production, and applications, J. Audio Eng. Soc. **35**, 760-777 (1987). https://www.aes.org/e-lib/browse.cfm?elib=5181

[12] G.F. Vander Voort, ed., ASM Handbook: Volume 9 Metallography and Microstructures, ASM international, Ohio, 2004.

[13] D.W. Dietrich, ed., ASM Handbook: Volume 92: Properties and Selection: Nonferrous Alloys and Special-Purpose Materials, ASM International, 1990. DOI: https://doi.org/10.31399/asm.hb.v02.9781627081627

[14] J.R. Davis, ed., ASM Specialty Handbook: Nickel, cobalt, and their alloys, ASM international, Ohio, 2000. DOI: https://doi.org/10.1361/ncta2000p003

[15] F.G. Hanejko, H.G. Rutz, C.G. Oliver, Effects of processing and materials on soft magnetic performance of powder metallurgy parts, in: Present. 1992 Powder Metall. World Congr., San Francisco, 1992: p. 375-403. www.hoeganaes.com.

[16] V. Tsakiris, M. Petrescu, Influence of purity and fabrication technology on the properties of soft magnetic Fe-50Ni alloy. Sci. Bull, Univ. Politeh. Bucharest. **69**, 67-78 (2007). DOI: https://doi.org/10.13140/2.1.3045.0564

[17] P. Vahdati Yekta, A. Ghasemi, E.M. Sharifi, Magnetic and mechanical properties of cold-rolled permalloy, J. Magn. Magn. Mater. **468**, 155-163 (2018). DOI: https://doi.org/10.1016/j.jmmm.2018.07.088

[18] A.T. English, G.Y. Chin, Metallurgy and magnetic properties control in permalloy. J. Appl. Phys. **38**, 1183-1187 (1967). DOI: https://doi.org/10.1063/1.1709532

[19] H.H. Scholefield, R.V. Major, B. Gibson, A.P. Martin, Factors influencing the initial permeability of some alloys based on 80Ni20Fe, J. Appl. Phys. **18**, 41-48 (1967). DOI: https://doi.org/10.1088/0508-3443/18/1/309

[20] T. Akomolafe, G.W. Johnson, The influence of texture on the magnetic permeability of 77 wt% Ni permalloys, J. Mater. Sci. **21**, 2403-2408 (1986). DOI: https://doi.org/10.1007/BF01114284

[21] E.G. Taylor, G.W. Johnson, The influence of molybdenum concentration on the magnetic permeability and kinetics of order formation in molybdenum permalloys, J. Mater. Sci. **12**, 51-60 (1977). DOI: https://doi.org/10.1007/BF00738471

[22] F. Pfeifer, C. Radeloff, Soft magnetic Ni-Fe and Co-Fe alloys – some physical and metallurgical aspects, J. Magn. Magn. Mater. **19**, 190-207 (1980). DOI: https://doi.org/10.1016/0304-8853(80)90592-2

[23] S. Hasani, M. Shamaniana, A. Shafyeia, P. Behjati, J.A. Szpunar, M. Fathi-Moghaddam, Nano/sub-micron crystallization of Fe-Co-7.15V alloy by thermo-mechanical process to improve magnetic properties, Mater. Sci. Eng. B Solid-State Mater. Adv. Technol. **190**, 96-103 (2014). DOI: https://doi.org/10.1016/j.mseb.2014.09.013

[24] S. Preston, G.W. Johnson, Effect of grain size and orientation on the initial permeability of 36 wt % Ni-Fe alloys. J. Mater. Sci. **19**, 4099-4105 (1984). DOI: https://doi.org/10.1007/BF00980777

[25] D.A. Colling, R.G. Aspden, Influence of sulfur on initial permeability of commercial 49% Ni-Fe alloys, J. Appl. Phys. **40**, 1571-1572 (1969). DOI: https://doi.org/10.1063/1.1657775

[26] S. Hasani, M. Shamanian, A. Shafyei, P. Behjati, M. Nezakat, M. Fathi-Moghaddam, J.A. Szpunar, Influence of annealing treatment on micro/macro-texture and texture dependent magnetic properties in cold rolled FeCo-7.15V alloy, J. Magn. Magn. Mater. **378**, 253-260 (2015). DOI: https://doi.org/10.1016/j.jmmm.2014.11.050

[27] R.T. Casani, W.A. Klawitter, A.A. Lykens, F.W. Ackermann, Secondary recrystallization in high-purity 49% Ni-Fe, J. Appl. Phys. **37**, 1202-1204 (1966). DOI: https://doi.org/10.1063/1.1708393

[28] M. Stefán, G. Hatta, P. Arató, On the secondary recrystallization and magnetic properties of Fe-Ni alloys, J. Magn. Magn. Mater. **19**, 208-210 (1980). DOI: https://doi.org/10.1016/0304-8853(80)90593-4

[29] M. Nabialek, B. Jez, K. Jez, K. Bloch, Structural and magnetic properties of the rapid cooled alloys: Fe60Co10Y5 + xZr5-xB20 (where: x = 0 or 2), Rev. Chim. **70**, 224-227 (2019). DOI: https://doi.org/10.37358/RC.19.1.6887

[30] J. Zbroszczyk, J. Olszewski, W. Ciurzyńska, M. Nabiałek, P. Pawlik, M. Hasiak, A. Łukiewska, K. Perduta, Glass-forming ability and magnetic properties of bulk (or 2, Nb, Ti) alloys, J. Magn. Magn. Mater. **304**, e724-e726 (2006). DOI: https://doi.org/10.1016/j.jmmm.2006.02.203

[31] K. Błoch, M. Nabiałek, P. Postawa, A.V. Sandu, A. Śliwa, B. Jeż, The magnetisation process of bulk amorphous alloys: Fe36 + xCo36−xY8B20, where: x = 0, 3, 7, or 12, Materials (Basel). **13**, 846 (2020). DOI: https://doi.org/10.3390/ma13040846

[32] M. Nabiałek, B. Jeż, K. Błoch, J. Gondro, K. Jeż, A.V. Sandu, P. Pietrusiewicz, Relationship between the shape of X-ray diffraction patterns and magnetic properties of bulk amorphous alloys Fe65Nb5Y5 + xHf5-xB20 (where: x = 0, 1,2, 3, 4, 5), J. Alloys Compd. **820**, 153420 (2020). DOI: https://doi.org/10.1016/j.jallcom.2019.153420

[33] M. Nabiałek, B. Jeż, K. Błoch, The influence of the silicon content on the formation of Fe23B6 metastable phases in Fe65Co11−xB-20SixZr2Hf2 bulk amorphous alloys, Metall. Mater. Trans. A. **51**, 4602-4609 (2020). DOI: https://doi.org/10.1007/s11661-020-05894-y

[34] K. Jeż, M. Nabiałek, S. Walters, A.V. Sandu, B. Jeż, The influence of Nb and Mo content on the magnetisation process of bulk amorphous alloys based on Fe, Acta Phys. Pol. A. **138**, 196-199 (2020). DOI: https://doi.org/10.12693/APhysPolA.138.196

[35] R.D. Enoch, A. Winterborn, Magnetic characteristics of a high-permeability Ni-Fe-Cu-Mo alloy, J. Appl. Phys. **18**, 1407-1413 (1967). DOI: https://doi.org/10.1088/0508-3443/18/10/306

[36] K. Aoyagi, Variations of crystal magnetic anisotropy of Mo-Fe-Ni alloys with heat treatments, Jpn. J. Appl. Phys. **4**, 551-556 (1965). DOI: https://doi.org/10.1143/JJAP.4.551

[37] L.J. Li, R.W. Shao, Effect of heat treatment on the structure and mechanical properties of the hot-rolling plate of Fe-42% Ni (4J42), Adv. Mater. Res. **194-196**, 321-325 (2011). DOI: https://doi.org/10.4028/www.scientific.net/AMR.194-196.321

[38] I. Mazurina, T. Sakai, H. Miura, O. Sitdikov, R. Kaibyshev, Grain refinement in aluminum alloy 2219 during ECAP at 250°C, Mater. Sci. Eng. A. **473**, 297-305 (2008). DOI: https://doi.org/10.1016/j.msea.2007.04.112

[39] C.S. Barrett, Structure of iron after compression, Trans. Aime. **135**, 296-326 (1939).

[40] A. Rollett, F. Humphreys, G.S. Rohrer, M. Hatherly, Recrystallization and related annealing phenomena: Second Edition, Elsevier, 2004. DOI: https://doi.org/10.1016/B978-0-08-044164-1.X5000-2

[41] R.D. Doherty, Recrystallization and texture. Prog. Mater. Sci. **42**, 39-58 (1997). DOI: https://doi.org/10.1016/s0079-6425(97)00007-8

[42] P.A. Beck, Annealing of cold worked metals, Adv. Phys. **3**, 245-324 (1954). DOI: https://doi.org/10.1080/00018735400101203

[43] M.B. Bever, D.L. Holt, A.L. Titchener, The stored energy of cold work, Prog. Mater. Sci. **17**, 5-177 (1973). DOI: https://doi.org/10.1016/0079-6425(73)90001-7

[44] F. Adcock, The internal mechanism of cold-work and recrystallization in Cupro-Nickel, J. Inst. Met. **27**, 73-92 (1922).

[45] P.S. Mathur, W.A. Backofen, Mechanical contributions to the plane-strain deformation and recrystallization textures of aluminum-killed steel, Metall. Trans. **4**, 643-651 (1973). DOI: https://doi.org/10.1007/BF02643069

[46] G.E. Dieter, Mechanical metallurgy (2001), SI Metr. Ed. (1988).

[47] I.L. Dillamore, W.T. Roberts, Rolling textures in f.c.c. and b.c.c. metals, Acta Metall. **12**, 281-293 (1964). DOI: https://doi.org/10.1016/0001-6160(64)90204-4

[48] R.E. Smallman, D. Green, The dependence of rolling texture on stacking fault energy, Acta Metall. **12**, 145-154 (1964). DOI: https://doi.org/10.1016/0001-6160(64)90182-8

[49] S. Dey, N. Gayathri, M. Bhattacharya, P. Mukherjee, In Situ XRD Studies of the Process Dynamics During Annealing in Cold-Rolled Copper, Metall. Mater. Trans. A. **47**, 6281-6291 (2016). DOI: https://doi.org/10.1007/s11661-016-3768-0

[50] A.S. Malin, M. Hatherly, Microstructure of cold-rolled copper, Met. Sci. **13**, 463-472 (1979). DOI: https://doi.org/10.1179/030634579790438363

[51] M.K. Banerjee, 2.1 Fundamentals of Heat Treating Metals and Alloys, in: Compr. Mater. Finish., Elsevier, 2017: pp. 1-49. DOI: https://doi.org/10.1016/B978-0-12-803581-8.09185-2

[52] R.S. Sundar, S.C. Deevi, Soft magnetic FeCo alloys: alloy development, processing, and properties, Int. Mater. Rev. **50**, 157-192 (2005). DOI: https://doi.org/10.1179/174328005X14339

[53] X. Zhong, L. Huang, F. Liu, Discontinuous dynamic recrystallization mechanism and twinning evolution during hot deformation of Incoloy 825, J. Mater. Eng. Perform. **29**, 6155-6169 (2020). DOI: https://doi.org/10.1007/s11665-020-05093-1

[54] M. Amir, H. Gungunes, A. Baykal, M.A. Almessiere, H. Sözeri, I. Ercan, M. Sertkol, S. Asiri, A. Manikandan, Effect of annealing temperature on magnetic and mössbauer properties of ZnFe2O4 nanoparticles by sol-gel approach, J. Supercond. Nov. Magn. **31**, 3347-3356 (2018). DOI: https://doi.org/10.1007/s10948-018-4610-2

[55] S. Asiri, M. Sertkol, H. Güngüneş, M. Amir, A. Manikandan, İ. Ercan, A. Baykal, The temperature effect on magnetic properties of NiFe2O4 nanoparticles, J. Inorg. Organomet. Polym. Mater. **28**, 1587-1597 (2018). DOI: https://doi.org/10.1007/s10904-018-0813-z

[56] J. Huber, M. Hatherly, Nucleation of recrystallized grains in heavily cold-worked α-brass, Met. Sci. 13, 665-669 (1979). DOI: https://doi.org/10.1179/030634579790434268

[57] R.K. Ray, W.B. Hutchinson, B.J. Duggan, A study of the nucleation of recrystallization using HVEM, Acta Metall. **23** (1975) 831-840. DOI: https://doi.org/10.1016/0001-6160(75)90199-6

[58] R.L. Fullman, J.C. Fisher, Formation of Annealing Twins During Grain Growth, J. Appl. Phys. **22**, 1350-1355 (1951). DOI: https://doi.org/10.1063/1.1699865

[59] W.W. Mullins, The effect of thermal grooving on grain boundary motion, Acta Metall. **6**, 414-427 (1958). DOI: https://doi.org/10.1016/0001-6160(58)90020-8

[60] R.E. Reed-Hill, R. Abbaschian, R. Abbaschian, Physical metallurgy principles, Van Nostrand New York, 1973.

[61] T. Hosoda, Microstructure and texture evolution in cold-rolled and annealed alloy MA-956, Colorado School of Mines, 2014. https://www.proquest.com/docview/1609182152

[62] S. Hasani, M. Shamanian, A. Shafyei, M. Nezakat, H. Mostaan, J.A. Szpunar, Effect of recrystallization and phase transitions on the mechanical properties of semihard magnetic FeCo-7.15 V alloy during the thermomechanical process, Metall. Mater. Trans. A Phys. Metall. Mater. Sci. **48**, 1903-1909 (2017). DOI: https://doi.org/10.1007/s11661-017-3954-8

[63] S. Hasani, M. Shamanian, A. Shafyei, P. Behjati, H. Mostaan, P. Sahu, J.A. Szpunar, Electron microscopy study on grain boundary characterizations of Fe-Co-V alloy during annealing, Vacuum **114**, 1-5 (2015). DOI: https://doi.org/10.1016/j.vacuum.2014.12.025

[64] S. Hasani, A. Shafyei, M. Nezakat, H. Mostaan, P. Behjati, P. Sahu, The effect of the order-disorder transition on the electrical, magnetic and mechanical properties of Vicalloy I, Intermetallics **81**, 73-79 (2017). DOI: https://doi.org/10.1016/j.intermet.2017.02.027

[65] M.R. Kamali, A.R. Mashreghi, L.P. Karjalainen, S. Hasani, V. Javaheri, S. Saukko, J. Kömi, Reobservations on ordering, precipitation and polymorphic phase transformation phenomena during annealing of a severely cold rolled magnetic Fe-Co-10V alloy, Materialia. **12**, 100765 (2020). DOI: https://doi.org/10.1016/j.mtla.2020.100765

[66] M.R. Kamali, L.P. Karjalainen, A.R. Mashregi, S. Hasani, V. Javaheri, J. Kömi, Reobservations of ferrite recrystallization in a cold-rolled ordered Fe-50Co-10V alloy using the EBSD method, Mater. Charact. **158**, 109962 (2019). DOI: https://doi.org/10.1016/j.matchar.2019.109962

[67] R.J. Willey, Formation of the K-state in a Ni-Fe-Mo-Cu alloy, J. Mater. Sci. **13**, 871-875 (1978). DOI: https://doi.org/10.1007/BF00570526

[68] I.V. Vernyhora, V.A. Tatarenko, S.M. Bokoch, Thermodynamics of fcc-Ni-Fe alloys in a static applied magnetic field, ISRN Thermodyn. 2012, 1-11 (2012). DOI: https://doi.org/10.5402/2012/917836

[69] A. Vidoz, D. Lazarević, R. Cahn, Strain-ageing of ordering alloys, with special reference to the nickel-iron system, Acta Metall. **11**, 17-33 (1963). DOI: https://doi.org/10.1016/0001-6160(63)90121-4

[70] R.C. Jackson, E.W. Lee, Magnetic and electrical properties of 77-14-5-4 wt % Ni-Fe-Cu-Mo and related alloys, J. Mater. Sci. **1**, 362-366 (1966). DOI: https://doi.org/10.1007/BF00549934

[71] H. Mostaan, M. Shamanian, S.M. Monirvaghefi, P. Behjati, S. Hasani, M. Fathi Moghaddam, M. Amiri, J.A. Szpunar, Analysis and characterization of microstructural evolutions, mechanical response and fracture mechanism of laser welded Fe-Co-V ultra-thin foils, Opt. Laser Technol. **68**, 211-219 (2015). DOI: https://doi.org/10.1016/j.optlastec.2014.12.003

[72] E. Orowan, Fracture and strength of solids, Reports Prog. Phys. **12**, 309 (1949). DOI: https://doi.org/10.1088/0034-4885/12/1/309

[73] R.H. Van Stone, T.B. Cox, J.R. Low, J.A. Psioda, Microstructural aspects of fracture by dimpled rupture, Int. Met. Rev. **30**, 157-180 (1985). DOI: https://doi.org/10.1179/imtr.1985.30.1.157

[74] D.A. Shockey, L. Seaman, K.C. Dao, D.R. Curan, A Computational Fracture Model for SA533, Grade B, Class i Steel Based upon Microfracture Process, EPRI Ductile Fract. Res. Rev. Doc. EPRI NP-701-SR. (1978).

[75] A.J. Birkle, R.P. Wei, G.E. Pellissier, Analysis of plain-strain fracture in a series of 0.45C-Ni-Mo steels with different sulfur contents, Trans. ASM. **59**, 981 (1966).

[76] C.D. Beachem, Electron fractographic studies of mechanical fracture processes in metals, J. Fluids Eng. Trans. ASME. **87**, 299-306 (1965).
DOI: https://doi.org/10.1115/1.3650544

[77] M. Reihanian, F.K. Hadadian, M.H. Paydar, Fabrication of Al-2 vol% Al2O3/SiC hybrid composite via accumulative roll bonding (ARB): An investigation of the microstructure and mechanical properties, Mater. Sci. Eng. A. **607**, 188-196 (2014).
DOI: https://doi.org/10.1016/j.msea.2014.04.013

[78] R.W. Hertzberg, R.P. Vinci, J.L. Hertzberg, Deformation and fracture mechanics of engineering materials, John Wiley & Sons, 2020.

[79] R.H. Yu, S. Basu, Y. Zhang, A. Parvizi-Majidi, J.Q. Xiao, Pinning effect of the grain boundaries on magnetic domain wall in FeCo-based magnetic alloys, J. Appl. Phys. **85**, 6655 (1999). DOI: https://doi.org/10.1063/1.370175

[80] R.H. Yu, S. Basu, L. Ren, Y. Zhang, A. Parvizi-majidi, K.M. Unruh, J.Q. Xiao, High Temperature Soft Magnetic Materials: FeCo Alloys and Composites, IEEE Trans. Magn. **36**, 3388-3393 (2000). DOI: https://doi.org/10.1109/20.9088099

[81] T. Sourmail, Evolution of strength and coercivity during annealing of FeCo based alloys, Scr. Mater. **51**, 589-591 (2004).
DOI: https://doi.org/10.1016/j.scriptamat.2004.05.028

[82] B. Nabi, A.-L. Helbert, F. Brisset, G. André, T. Waeckerlé, T. Baudin, Effect of recrystallization and degree of order on the magnetic and mechanical properties of soft magnetic FeCo-2V alloy, Mater. Sci. Eng. A. **578**, 215-221 (2013).
DOI: https://doi.org/10.1016/j.msea.2013.04.066